Unraveling pairon excitations and the antiferromagnetic contributions in the cuprate specific heat

Yves Noat, Alain Mauger, William Sacks

Unraveling pairon excitations and the antiferromagnetic contributions in the cuprate specific heat

Yves Noat*,[1] Alain Mauger,[2] and William Sacks[2,3]

[1] *Institut des Nanosciences de Paris, CNRS, UMR 7588 Sorbonne Université, Faculté des Sciences et Ingénierie, 4 place Jussieu, 75005 Paris, France*
[2] *Institut de Minéralogie, de Physique des Matériaux et de Cosmochimie, CNRS, UMR 7590, Sorbonne Université, Faculté des Sciences et Ingénierie, 4 place Jussieu, 75005 Paris, France*
[3] *Research Institute for Interdisciplinary Science, Okayama University, Okayama 700-8530, Japan*

(Dated: August 7, 2024)

Thermal measurements, such as the entropy and the specific heat, reveal key elementary excitations for understanding the cuprates. In this paper, we study the specific heat measurements on three different compounds $La_{2-x}Sr_xCuO_4$, $Bi_2Sr_2CaCu_2O_{8+\delta}$ and $YBa_2Cu_3O_{7-\delta}$ and show that the data are compatible with 'pairons' and their excitations. However, the precise fits require the contribution of the antiferromagnetic entropy deduced from the magnetic susceptibility $\chi(T)$.

Two temperature scales are involved in the excitations above the critical temperature T_c: the pseudogap T^*, related to pairon excitations, and the magnetic correlation temperature, T_{max}, having very different dependencies on the carrier density (p). In agreement with our previous analysis of $\chi(T)$, the $T_{max}(p)$ line is not the signature of a gap in the electronic density of states, but is rather the temperature scale of strong local antiferromagnetic correlations which dominate for low carrier concentration. These progressively evolve into paramagnetic fluctuations in the overdoped limit.

Our results are in striking contradiction with the model of J. L. Tallon and J. G. Storey [Phys. Rev. B **107**, 054507 (2023)], who reaffirm the idea of a T-independent gap E_g, whose temperature scale $T_g = E_g/k_B$ decreases linearly with p and vanishes at a critical value $p_c \sim 0.19$.

Finally, we discuss the unconventional fluctuation regime above T_c, which is associated with a mini-gap $\delta \sim 2\,\text{meV}$ in the pairon excitation spectrum. This energy scale is fundamental to the condensation mechanism.

PACS numbers: 74.72.h,74.20.Mn,74.20.Fg

INTRODUCTION

The measurement of the specific heat is a direct probe of thermal excitations of a system. In the case of a conventional superconductor, with negligible phonon contributions at low temperature, the excitations are intimately linked to the nature of the condensation (see Ref. [1] for a review). In the conventional case, described by the Bardeen-Cooper-Schrieffer (BCS) theory [2], elementary excitations are of the fermionic type, the quasiparticles, as illustrated in Fig. 1. Moreover, the good agreement between theory and experiment is striking, as in Fig. 2 from Ref.[3].

The breaking of Cooper pairs gives rise to quasiparticles having the dispersion relation $E_k = \sqrt{\epsilon_k^2 + \Delta^2}$. The occupation of quasiparticle states, given by the Fermi-Dirac statistics, increases with temperature giving rise to a decrease of the superconducting (SC) gap, which finally vanishes at T_c (inset of Fig. 3, upper panel). Above T_c the normal metallic state is fully recovered. It follows that there is a discontinuity in the entropy slope and a corresponding jump in the specific heat as shown in Figs. 2 and 3. This is characteristic of a second order phase transition and the vanishing of the order parameter, the energy gap, at the critical temperature.

The situation is very different in cuprates where multiple degrees of freedom are likely to be superposed (phonons, magnons, pair excitations etc.) at the relevant temperatures. Several theoretical works have addressed the difficult task to study the thermodynamic properties, pointing out the important role of the pseudogap and pair degrees of freedom above T_c [4–6]. Although these contributions explore interesting concepts, so far they remain inconclusive.

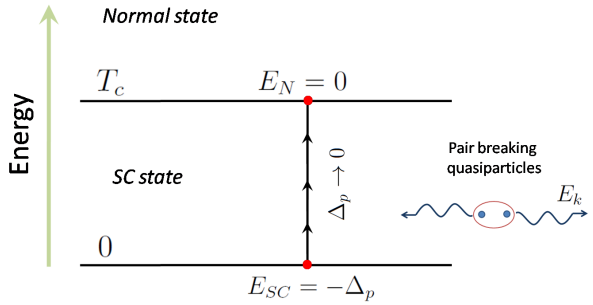

FIG. 1. (Color online) Excitation process in a conventional superconductor described by BCS theory [2]. Breaking a Cooper pair gives rise to two quasiparticles with energy E_k. The excitation is of fermionic type. As the temperature increases, more and more quasiparticles are created (pair breaking) leading to the decreasing of the gap $\Delta_p(T)$. The normal state is recovered at the critical temperature T_c, where $\Delta_p(T_c) = 0$.

In a previous work, we have calculated the contribution of pairon excitations in the superconducting state as well as above T_c. The relevant energy diagram is now shown in Fig. 4. The observed shape of the specific

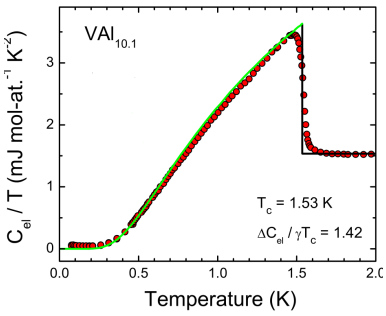

FIG. 2. (Color online) Experimental $\frac{C_v}{T}$ (red dots) measured in $VAl_{10.1}$ by Klimczuk et al. (adapted from Ref.[3]). Continuous line: Excellent fit using BCS theory (see Ref. [3] for details).

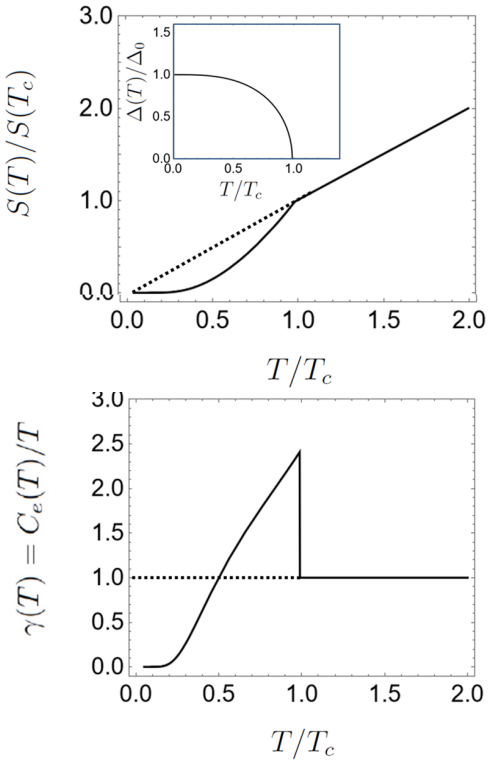

FIG. 3. (Color online) Upper panel: Normalized entropy as a function of temperature in the framework of the BCS theory [2]. Inset: Normalized gap $\Delta(T)/\Delta_0$, where Δ_0 is the gap at $T = 0$, as a function of temperature. Lower panel: Coefficient $\gamma(T) = C_v(T)/T$ calculated in the framework of the BCS theory. Note that the normal γ_N is recovered above T_c.

heat strongly depends on the carrier concentration [7–10], as illustrated in Fig. 5, where the general evolution of the temperature dependent $\gamma(T)$ coefficient is shown for 5 different concentrations ranging from the underdoped to the overdoped regimes. In the underdoped regime, above T_c, $\gamma(T)$ is well below the normal state value up to very high temperatures. This effect disappears in the overdoped regime, and can even invert (upper curves in Fig. 5). In addition, in the whole doping range, there is

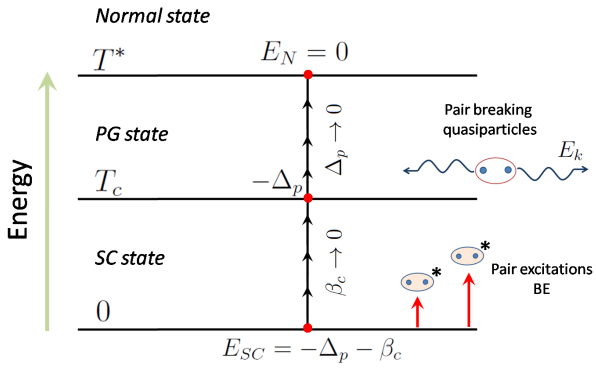

FIG. 4. (Color online) Upper panel: Excitation processes in a cuprate superconductor in the framework of the pairon model [12]. At low temperature, the dominant excitations are pairon (bosonic) excitations. The diagram is simplified in the underdoped case where pair excitations dominate below T_c and quasiparticle excitations dominate above T_c. In the general case, pair breaking quasiparticles can exist below T_c. However, the critical temperature is still defined by the vanishing of the pairon correlation energy β_c and the pseudogap temperature T^* is defined by the vanishing of the pairing gap.

no sharp discontinuity in $C_v(T)$ at T_c, as expected in the BCS scenario (see Fig. 3). Instead, an exponential tail is observed in cuprates above T_c on a typical temperature scale $\sim 5 - 10K$ [8–11] for LSCO and twice that for BSCO, which is one order of magnitude above the fluctuations within the Ginzburg-Landau theory [11, 13].

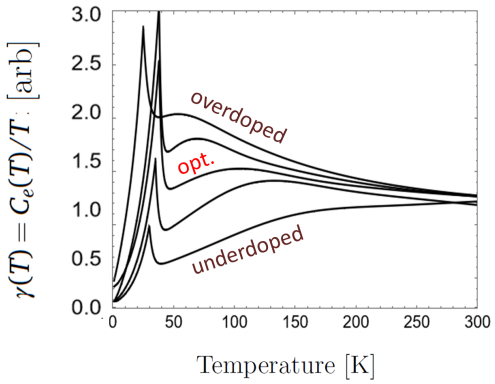

FIG. 5. (Color online) General shape of $\gamma(T)$ coefficient for different doping values from underdoped to the overdoped regime using our phenomenological model described in the text. Notice the continuous evolution of the background slope above T_c and the hump position.

In the underdoped regime, even at high temperatures, the normal metallic state is not recovered. Instead, the entropy is roughly linear at high temperature ($T \gtrsim 200K$), but below the expected normal state line. This effect has been interpreted by Tallon et al. in terms of a temperature-independent gap E_g in the density of states [14–16]. In the specific heat, the latter is found to decrease with carrier density and vanishes at

a critical value $p_c = 0.19$. However, this is in direct contradiction with tunneling and photoemission spectroscopic measurements (see [17–20] for reviews), where the pseudogap depends on temperature, vanishes at T^*, and which does not cross the SC dome.

In a previous article, we calculated the electronic contribution to the specific heat in the framework of the pairon model [12]. Two temperature scales are relevant, the critical temperature T_c, as expected, and the pseudogap temperature, T^*, at which the electronic state returns to the normal metallic state. In the present article, we extend this work to include two major effects: the magnetic excitations and the fluctuations above T_c. This allows to do precise fits of the specific heat of different materials $La_{2-x}Sr_xCuO_4$ (LSCO), $Bi_2Sr_2CaCu_2O_{8+\delta}$ (BSCCO) and $YBa_2Cu_3O_{7-\delta}$ (YBCO), see Fig. 6. In particular, we show that in addition to T_c and T^*, there is a third temperature scale $T_{max} \sim J/k_B$, the characteristic temperature of antiferromagnetic (AF) correlations, where J is the AF exchange energy, in agreement with our study of magnetic susceptibility [21], as well as pioneering works [22–24].

From this analysis, the behavior of the entropy in the underdoped regime described above is due to the magnetic contribution and not to a gap in the electronic excitations. This is in stark contradiction with the conclusions advanced by Tallon and Storey [25] who rule out the existence of excited pairons in the specific heat.

THE PAIRON MODEL

The following important issues are still under debate in cuprates:

- the pairing mechanism,
- the nature of the pseudogap and its relation to superconducting order,
- the mechanism leading to the SC condensation,
- and the dependence of the physical parameters on carrier concentration.

These issues can be addressed in the framework of our pairon model. First, we have proposed that in cuprates, hole pairs, or pairons, are formed below the characteristic temperature T^* due to the persistence of local magnetism on a typical scale ξ_{AF}, the antiferromagnetic (AF) correlation length [26]. Their binding energy is directly related to the effective AF exchange energy J_{eff} due to the local magnetic order surrounding the pairon. At low temperature, pairons condense in a collective quantum state as a result of their mutual interactions [27].

There are two fundamental energy scales, the antinodal energy gap Δ_p, associated with pair formation, and the coherence energy β_c, associated with pair correlations. These two energies are proportional to the two temperature scales T^*, the pseudogap temperature, and T_c, the critical temperature, respectively [28]:

$$\begin{aligned} \Delta_p &= 2.2\, k_B\, T^* \\ \beta_c &= 2.2\, k_B\, T_c \end{aligned} \tag{1}$$

The pseudogap temperature T^* corresponds to the onset temperature of pairon formation while the critical temperature T_c corresponds to the onset of pairon-pairon correlations.

In addition, in our view, the pseudogap and the superconducting order are intimately linked [28]. Indeed, we have shown that T^* and T_c can be expressed as follows [29], in terms of the hole concentration:

$$\begin{aligned} T^* &= \alpha_1\,(1-p') \\ T_c &= \alpha_2\, p'(1-p') \end{aligned} \tag{2}$$

where the reduced density is:

$$p' = \frac{p - p_{min}}{p_{max} - p_{min}}$$

with $p_{min} = 0.05$, the minimum doping value and $p_{max} = 0.27$, the end of the SC dome. λ_i, $i = 1, 2$, are constants.

For BSCCO, the above relations are in very good agreement with experiments. Within the experimental resolution, we found $\alpha_1 \simeq \alpha_2 \approx 390\,\mathrm{K}$. For LSCO α_1 and α_2 are found to have slightly different values [29] ($\alpha_1/\alpha_2 = 1.25$ with $\alpha_1 = 200\,\mathrm{K}$). Both α_1 and α_2 are proportional to the same energy, J_{eff}.

At zero temperature, pairons form an ordered SC state. At finite temperature, they are excited in higher pair energy states. In addition, excited pairons can decay into quasiparticles. Thus, both bosonic (excited pairs) and fermionic (quasiparticles) excitations are present [12], as illustrated in Fig. 4. Contrary to the BCS case, the energy gap is not the order parameter. Indeed, since pairons exist above T_c, the critical temperature (and therefore the order parameter) is determined by pairon-pairon correlations, leading to the T_c dome [28]. Although the pair excitations follow Bose-Einstein statistics, the T_c is not determined by the standard expression for non-interacting bosons. Rather, the condensate density, which is proportional to the correlation energy $\beta_c(T)$ [27], is the true SC order parameter.

So far this model fits very well the $T_c(p)$ and $T^*(p)$ phase diagram, and fits quantitatively many experiments such as tunneling [27, 30] ARPES [31, 32] and magnetic susceptibility [21].

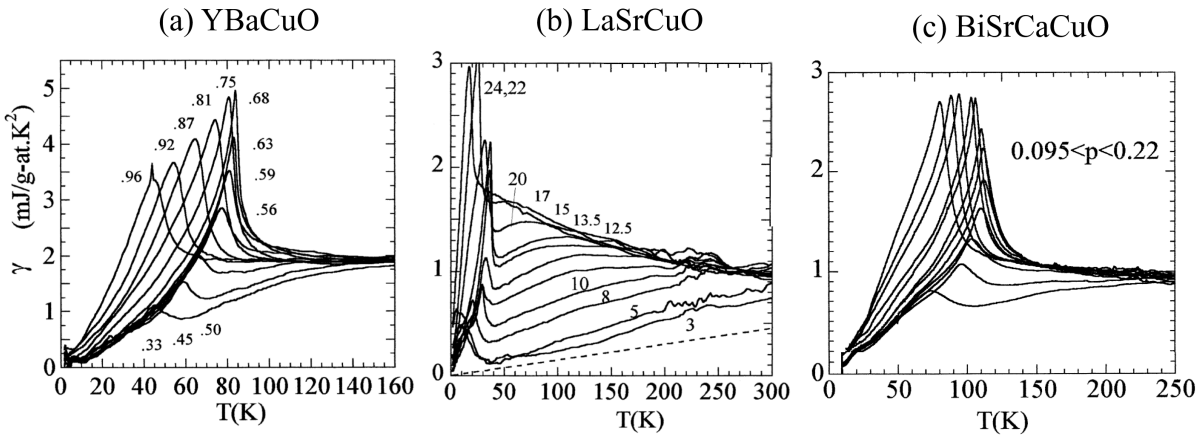

FIG. 6. (Color online) Experimental $\gamma(T)$ coefficient measured in three different compounds [15], $YBa_2Cu_3O_{7-\delta}$ (panel a), $La_{2-x}Sr_xCuO_4$ (panel b), $Bi_2Sr_2CaCu_2O_{8+\delta}$ (panel c).

Entropy in the pairon model

In order to understand the shape of the experimental curves, we now recall the ingredients of the electronic entropy of pairons. The details of the calculation can be found in our previous article [12]. The entropy $S(T)$ results from the contribution of both bosonic and fermionic excitations. At finite temperature, pairons are excited out of the condensate, their occupation being given by the Bose-Einstein statistics. $S(T)$ can be written in a concise way:

$$S(T) = \sum_i n_i(\varepsilon_i, T) S_i(\varepsilon_i, T) \tag{3}$$

where n_i is the density of excited pairons with energy ε_i with the associated entropy term S_i. Since pairons are composite bosons, we have $n_i \propto f_{BE}(\varepsilon_i, T) P_0(\varepsilon_i)$, where $f_{BE}(\varepsilon) = 1/\left(\exp\left(\frac{\varepsilon-\mu_b}{k_B T}\right) - 1\right)$ is the Bose-Einstein distribution and $P_0(\varepsilon_i)$ is the excited pair density of states.

Each excited pairon with energy ε_i can decay into quasiparticles with energy E_k^i. Thus, S_i can be expressed as a sum over each quasiparticle contribution

$$S_i(\varepsilon_i, T) = \sum_{\vec{k}} S(E_k^i, T) \tag{4}$$

where $S(E_k^i, T)$ is the fermionic entropy associated with the quasiparticle of energy $E_k^i = \sqrt{\epsilon_k^2 + {\Delta_k^i}^2}$. The excited pairs are related to the pairing amplitudes via the equation: $\varepsilon_i = \Delta_k^i - \Delta_p$ (see [21] and [12]). As seen in Fig. 7, this entropy takes into account not only the transition at T_c, where the derivative of the entropy is discontinuous, but also the return to the normal state through the end of the pseudogap at T^* [12].

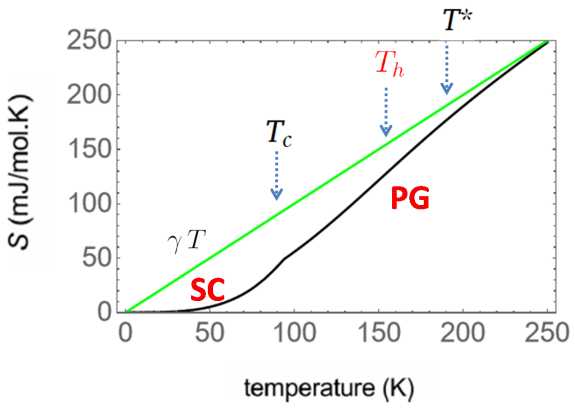

FIG. 7. (Color online) Plot of the entropy with temperature in the pairon model revealing the important temperature scales (values for BSCCO). The entropy has a discontinuous derivative at T_c due to the disappearance of the condensate but does not join the normal state $\gamma_N T$ line. A weak inflection above T_c is characterized by the temperature T_h. The normal state entropy is recovered at the pseudogap temperature T^*, indicating the vanishing of the pairing gap.

Fluctuations observed above T_c

A remarkable and general feature of the $\gamma(T)$ experimental curves is the prominent exponential decay just above the critical transition. We can extend the above calculation of $S(T)$ in a phenomenological way in order to take into account this fluctuation regime above T_c.

One approach, inspired by Ref. [33], is to consider a slightly modified chemical potential $\mu(T)$ which is smoothed on the scale of ΔT, as in Fig. 8. While phenomenological, it successfully accounts for boson interactions just above T_c. We use the same approach to include pairon-pairon correlations in the excited states to describe the fluctuation regime where the correlations persist. The fluctuation contribution, S_{fluct}, can be sim-

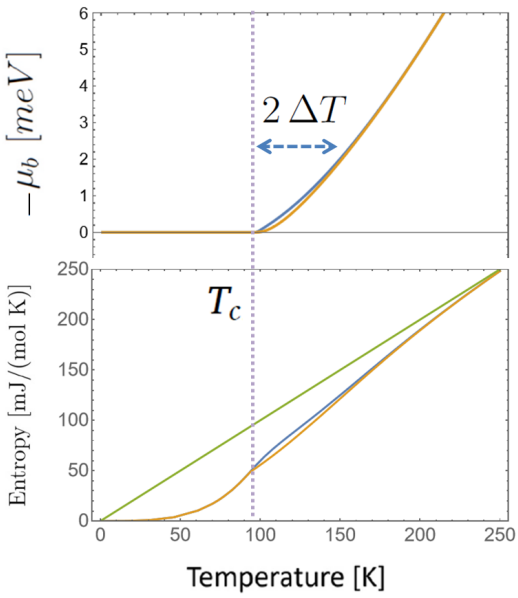

FIG. 8. (Color online) Upper panel: chemical potential (orange line) and modified chemical potential (blue line) including fluctuations in such a way that the entropy is smoothed above T_c on the scale ΔT (values for BSCCO). Lower panel: the corresponding entropy using the chemical potentials of the upper panel. With the standard chemical potential (orange line), the derivative of $S(T)$ is discontinuous at T_c while, with the modified chemical potential (blue line), it is continuous at T_c. Green line: normal state entropy.

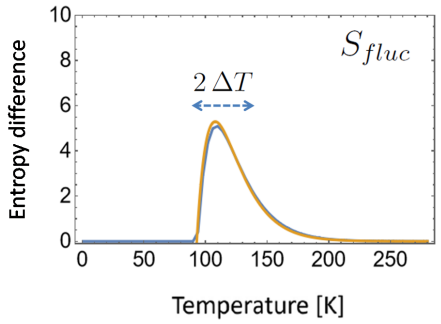

FIG. 9. (Color online) Fluctuation entropy S_{fluct} (blue curve) determined by subtracting the two entropy curves in Fig. 10. S_{fluct} sharply increases above T_c, reaches a maximum and then decreases rapidly on the typical temperature scale $\Delta T \sim 10 - 20K$ (values for BSCCO). Orange curve: S_{fluct} determined by the phenomenological expression, Eq. 7.

ply determined by subtracting the entropy with the standard chemical potential from the entropy with smoothed chemical potential, Fig. 9. The resulting specific heat, Fig. 10, shows an almost identical exponential decay as in the experiments.

The full calculation of the electronic entropy is done for three different hole concentrations, $p = 0.12$ (underdoped), $p = 0.16$ (optimally doped) and $p = 0.2$ (overdoped). As shown in Fig. 11, the $\gamma(T)$ coefficient exhibits

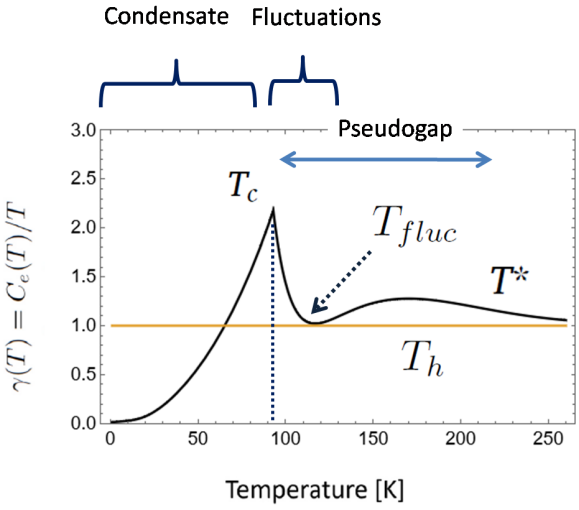

FIG. 10. (Color online) Electronic specific heat calculated in the framework of the pairon model, including the fluctuations. Three temperature scales can be distinguished above T_c: the fluctuation temperature T_{fluc}, the temperature of the hump T_h and the pseudogap temperature T^* where the normal state is recovered (values for BSCCO).

the expected peak at T_c due to the vanishing of the condensate. Just above the peak, the remarkable exponential tail extends from T_c on the characteristic temperature scale $\Delta T \sim 10K$, which we identify as the fluctuation regime. Beyond T_c, $\gamma(T)$ is still not constant as would be expected in the conventional case. Indeed, since excited pairs exist above T_c, the normal state is only recovered approaching T^*, which is well above T_c, especially in the underdoped case.

We also note that a clear hump is observed below T^* in $\gamma(T)$ at the characteristic temperature labeled by T_h. As described in our previous work [12], it corresponds to the inflection point in the energy gap function $\Delta_p(T)$. The latter physical parameter, fundamental to the model, expresses the density of excited pairons which decays with increasing temperature.

The values of the relevant parameters can be deduced by fitting the experimental data, which is generally a difficult task. To proceed, we introduce a simple phenomenological expression for the entropy, which is the sum of different contributions, the condensate and excited pairs terms, and the fluctuation term:

$$S_{elec} = S_{cond} + S_{pair} + S_{fluc} \tag{5}$$

where

$$S_{cond}(T) = S_{pair}(T)\, \mathrm{e}^{-N_c(T)/N_0}\ \Theta(T_c - T) \tag{6}$$

$$S_{fluc}(T) = A_{fluc}\,(T - T_c)\, \mathrm{e}^{-(T-T_c)/\Delta T}\ \Theta(T - T_c) \tag{7}$$

$$S_{pair}(T) = A_{pair} T\,(1 - \alpha_1\, \Delta(T)/\Delta_p)^{1/2} \tag{8}$$

Where A_{pair} and A_{fluc} are respectively the amplitudes of the pair term and the fluctuation term, and $\Theta(T)$ is the

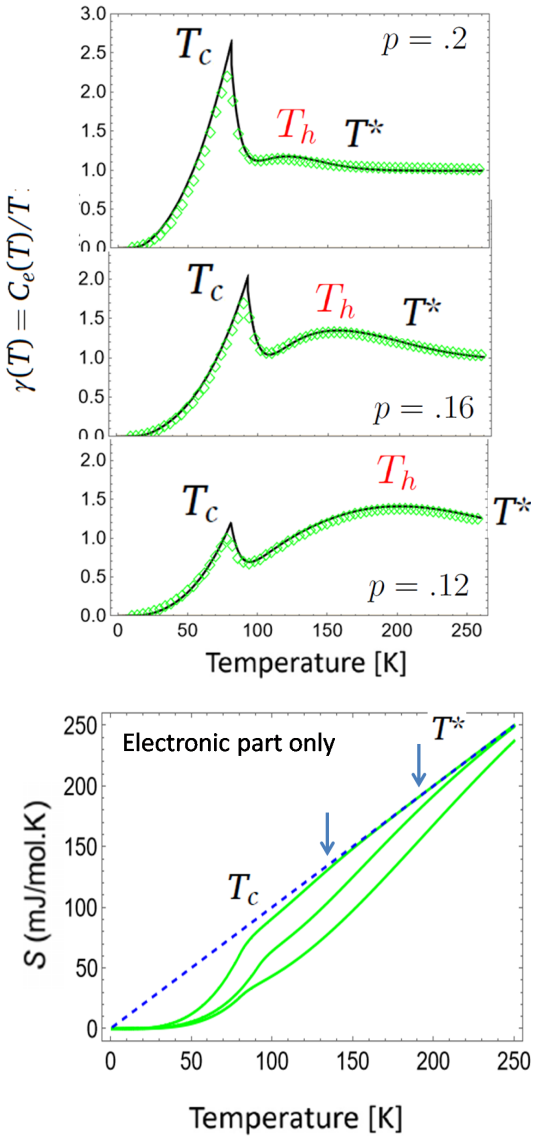

FIG. 11. (Color online) Temperature dependent entropy and $\gamma(T)$ coefficient calculated in the framework of the pairon model [12] (values for BSCCO). The modified chemical potential is used to include the fluctutions (see text).
Upper panel: $\gamma(T)$ coefficient for three different hole concentrations, underdoped ($p = 0.12$), optimally doped ($p = 0.16$), and overdoped ($p = 0.2$). The numerical solution (green points) is compared to the phenomenological expression (black line).
Lower panel: corresponding entropy for the same three hole concentrations.

standard Heaviside step function. Expression 5 can be directly compared to the numerical calculation (Fig. 11, upper panel). Obviously, the agreement is quite satisfactory.

As we will demonstrate, the fit to the experimental data requires the contribution of magnetic excitations. Adding the additional magnetic term, the total entropy is now:

$$S_{tot} = S_{cond} + S_{pair} + S_{fluc} + S_{AF} \tag{9}$$

The magnetic entropy can be deduced in a simple way: $S_{AF} = A_{mag} T \times \chi(T)$, where A_{mag} is the amplitude and $\chi(T)$ is the magnetic susceptibility of the 2D antiferromagnetic lattice, calculated in Ref. [34]. The AF susceptibility can be well described by the simplified expression [21]:

$$\chi(T) = \frac{1}{T + \frac{T_{max}^2}{T} + C} \tag{10}$$

where T_{max} is the characteristic temperature of magnetic correlations (where $\chi(T)$ is a maximum) and C is the Curie-Weiss constant. This simple temperature-dependent expression was shown to fit successfully the experimental magnetic susceptibility of cuprates as a function of carrier density [21].

ANALYSIS OF THE EXPERIMENTAL DATA

The case of LSCO

We now focus on the fitting and the analysis of experimental data. We first concentrate on the data obtained by Loram et al. in LSCO [15], see Fig. 6. The experimental $\gamma(T)$, and corresponding fits using the equation 9 for the entropy, are shown in Fig. 12 and Fig. 13. The agreement is very satisfactory for the whole doping range.

From the fits, we obtain the values of the parameters as a function of carrier concentration to deduce the phase diagram, Fig. 14. Above T_c, three temperature scales can be distinguished: the pseudogap temperature T^*, the magnetic temperature T_{max}, and the fluctuation temperature regime, corresponding to the exponential tail observed in $\gamma(T)$ between T_c and $T_{fluc} = T_c + \Delta T$.

The T^* determined from the fits corresponds roughly to the hump in the specific heat calculated using the numerical approach: $T_h \approx (2/3)T^*$. It decreases linearly with carrier concentration and extrapolates to zero at the end of the T_c dome at p_{max}. From this analysis, there is no indication of the T^* line crossing the dome.

The magnetic temperature behaves differently. It decreases linearly in the underdoped regime, clearly seen in Fig. 14. Remarkably, this linear behavior extrapolates to zero at $p \sim 0.2$ which is very close to the value found by Tallon et al. for the vanishing of their gap energy $E_g(p)$ [15]. However, the $T_{max}(p)$ curve derived from the fits deviates from linearity and levels off above optimum doping ($p \gtrsim .17$), as clearly seen in Fig. 14. A similar leveling off was deduced from our analysis of the magnetic susceptibility [21], in agreement with early pioneering works [23, 24]. In short, the analysis of the specific heat from LSCO confirms the $T_{max}(p)$ magnetic transition temperature in the phase diagram.

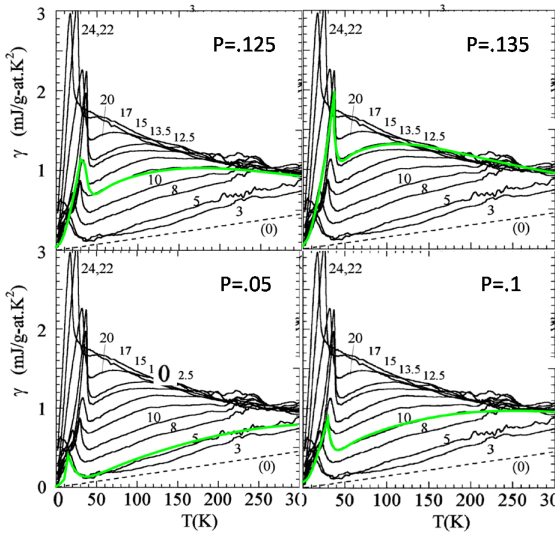

FIG. 12. (Color online) Experimental $\gamma(T)$ measured in $La_{2-x}Sr_xCuO_4$ [15]. Green lines: corresponding fits, in the underdoped regime, calculated with the phenomenological expression.

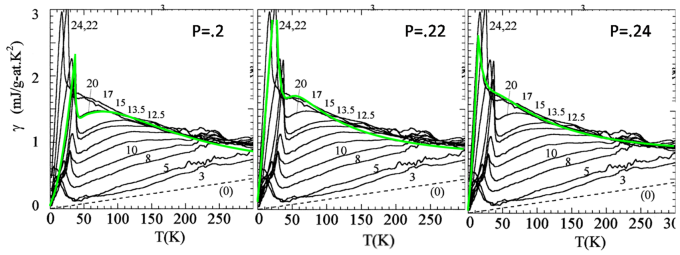

FIG. 13. (Color online) Experimental $\gamma(T)$ measured in $La_{2-x}Sr_xCuO_4$ [15] and corresponding fits in the overdoped regime (green lines).

Interestingly, the particular carrier concentration $p \sim 0.2$ also coincides with a suggested quantum critical point (see [35] and references therein). In our previous work ([21], [28]) we proposed that the particular slope of the $T_{max}(p)$ line, which extrapolates down to the same critical value, indicates the formation of 'simplons', or holes surrounded by 4 frozen spins in the 2D lattice. The symmetry properties of such spin-charge objects were explored further in our theoretical analysis [29], in particular their relation to pairon formation below T^*. Whether or not the 'simplon-pairon' model is compatible with some critical transition taking place at this special carrier density remains an open question.

Interpretation of the entropy

Given these results on the characteristic temperatures, we now interpret the specific heat and the entropy in a different light with respect to Tallon et al. [15, 16], who

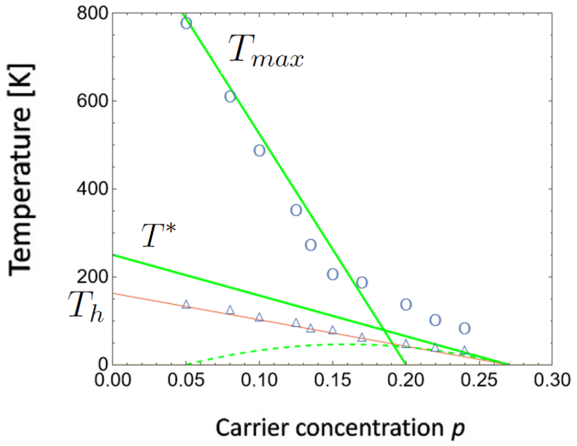

FIG. 14. (Color online) Phase diagram for $La_{2-x}Sr_xCuO_4$ deduced from the fits. Above T_c, the lines $T_{max}(p)$ and $T^*(p)$ are clearly distinct. The $T_{max}(p)$ line is in good agreement with the one deduced from the magnetic susceptibility [21]. From the fits we deduce $T_h(p)$ which follows $T^*(p)$ with a smaller slope $T_h(p) \approx \frac{2}{3}T^*(p)$ throughout the doping range.

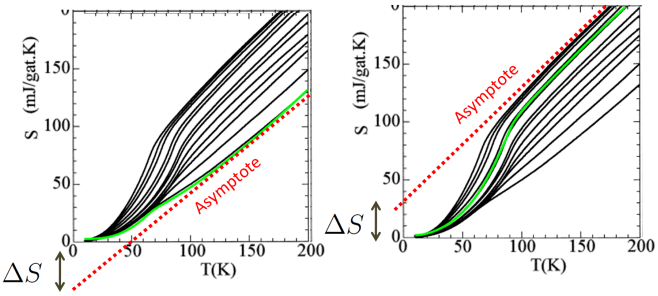

FIG. 15. (Color online) Left panel: entropy of $Bi_2Sr_2CaCu_2O_{8+\delta}$ in the underdoped regime (adapted from Ref. [15]). Right panel: entropy in the overdoped regime and corresponding fits (green lines). In the underdoped regime the asymptotic line (red dash line) is below the normal state $\gamma(T)$, while it is above in the overdoped regime (adapted from Ref. [15]). This entropy shift is due to the contribution of magnetic excitations and not to a gap in the electronic DOS, as described in the text.

have focused on YBCO (Fig. 6, panel (a)), and to some extent on BSCCO (panel (c)).

As mentioned previously, these authors consider the 'pseudogap' as being due to a constant electronic gap in the Fermi level DOS, at fixed p, of magnitude $E_g(p)$. In this model, one does not recover the entropy of the normal state $S(T) \sim \gamma T$ for large $T \gg T_c$. Instead, the entropy line is shifted to a lower value $S(T) \sim \gamma T - \Delta S$, as seen in Fig. 15, left panel for BSCCO. They deduce the gap energy from $E_g(p) \propto \Delta S/k_B$ and plot the corresponding phase diagram as a function of p. A similar $E_g(p)$ was also deduced from the magnetic susceptibility of LSCO and YBCO [36–38] which, according to their model, vanishes near $p_c \simeq 0.2$.

Several difficulties emerge from this interpretation:

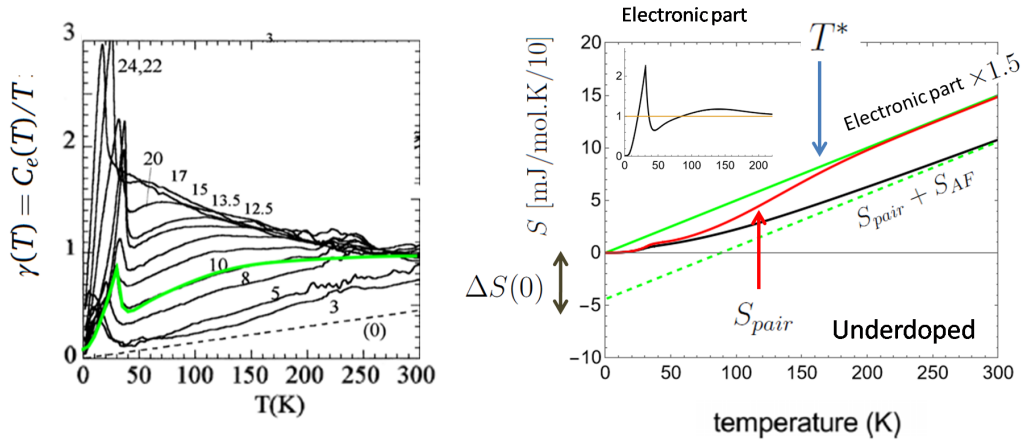

FIG. 16. (Color online) Left panel: experimental $\gamma(T)$ in the underdoped regime ($p = 0.1$) and corresponding fit (green line). Right panel: corresponding total entropy calculated from the fit (black line) and electronic part (red line). The magnetic term causes an apparent shift in the entropy. The apparent asymptotic line is below the normal $\gamma_N \times T$ entropy. Inset: corresponding electronic $\gamma(T)$ obtained by substracting the magnetic part.

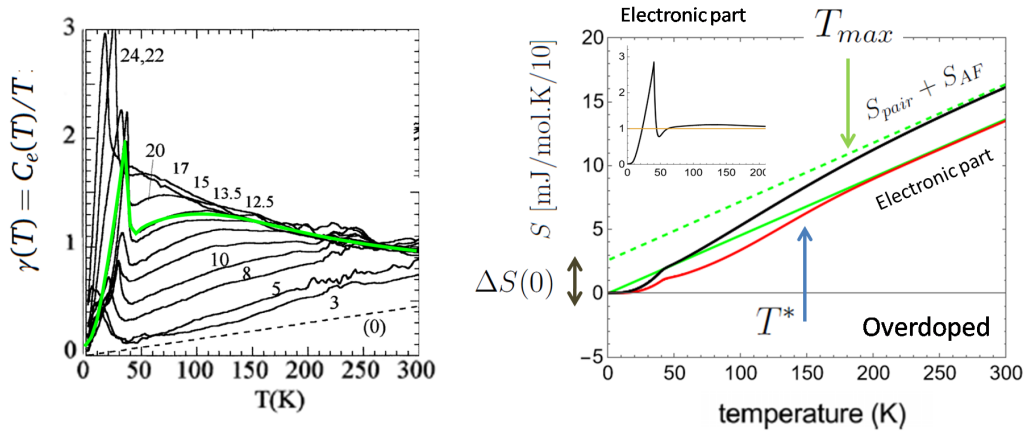

FIG. 17. (Color online) Left panel: experimental $\gamma(T)$ in the slightly overdoped regime (hole doping $p = 0.17$) and corresponding fit (green line). Left panel: corresponding entropy calculated from the fit (black line) and electronic part (red line). The apparent asymptotic line is above the normal $\gamma_N \times T$ entropy. Inset: corresponding electronic $\gamma(T)$ obtained by substracting the magnetic part.

firstly, the gap E_g does not close with rising *temperature* and secondly, the characteristic line $E_g(p)/k_B$ crosses the dome in the phase diagram. In addition, and perhaps most significantly, it fails to explain the behavior of $S(T)$ in the overdoped regime where ΔS becomes positive, as in Fig. 15, right panel. Indeed, a positive ΔS cannot be interpreted in terms of a 'gap' since E_g would have the wrong sign.

This question can be further explored thanks to the general formula Eq.9 for the entropy. Indeed, it confirms that the entropy shift, ΔS, is due to the magnetic part leading to the correct evolution of $S(T)$ with carrier density. In the case of BSCCO this conclusion is clearly illustrated in Fig. 15 where we have fitted the entropy from Loram et al. using the *identical equation* (9) as in the previous case of LSCO. For two contrasting hole concentrations, respectively in the underdoped and overdoped regimes, we see that the dashed red line illustrates well the asymptotes of the $S(T)$ curves. In the underdoped case, this line extrapolates to a negative ΔS at $T = 0$, while in the overdoped case, it extrapolates to a positive value. Clearly this entropy shift effect is continuous as a function of carrier density.

The general formula for $S(T)$ conveniently allows to separate the magnetic and electronic contributions to the total entropy. What's more, it allows to follow the $S(T)$ profile while varying the key parameters ($A_{pair}, A_{mag}, T^*, T_{max}$, etc.) around their 'best fit' values. This parameter tweaking can equally be done on the fits for Fig. 15, as well as the previous series of fits for LSCO, Figs. 12 and 13. Exploring the parameter space in this way gives a novel insight on the influence of the

AF magnetic term on the overall shape of the entropy above T_c.

In the pairon model the strictly electronic part of the entropy must return to the normal state, i.e. $\sim \gamma_N T$, once pairing vanishes at T^*. To confirm this important property, we return to the case of LSCO to extract the entropy terms in $S(T)$ using the equation (9). The electronic and magnetic terms of the entropy can be isolated from the best fits: underdoped case Fig. 16 and overdoped case Fig. 17. In the right panel of both figures, the black line corresponds to the total entropy, while the red line corresponds to the isolated electronic part.

Consider first the underdoped case, Fig. 16. The asymptotic dotted green line extrapolates to a negative value at $T = 0$, resulting in an apparent negative shift ΔS, as previously noted for BSCCO. Once the magnetic part is removed, the electronic part, red line, follows the expected behavior: the normal state is recovered above T^* due to pair breaking. To the contrary, in the overdoped case, Fig. 17, the asymptotic dotted line extrapolates to a positive ΔS value at $T = 0$. Again, once the magnetic part is removed, red curve, the normal state entropy is recovered above T^*.

To summarize, the change of the $S(T)$ asymptote from underdoped to overdoped is due to the magnetic $T\chi(T)$ term in the entropy, which depends strongly on the characteristic temperature T_{max}. In the underdoped regime, for $T < T_{max}$, the magnetic part gives rise to an additional contribution to the entropy $S \sim \gamma T - \Delta S$ in this temperature range. On the other hand, in the overdoped regime, the apparent entropy shift changes sign. The latter is thus not due to a constant (T-independent gap) in the electronic DOS, but to the contribution of magnetic excitations to the entropy. Moreover, for any carrier concentration, our results show that the strictly *electronic* part of the total $S(T)$ reveals the T-dependent pairing gap and has the normal $\sim \gamma_N T$ asymptote above T^* as required.

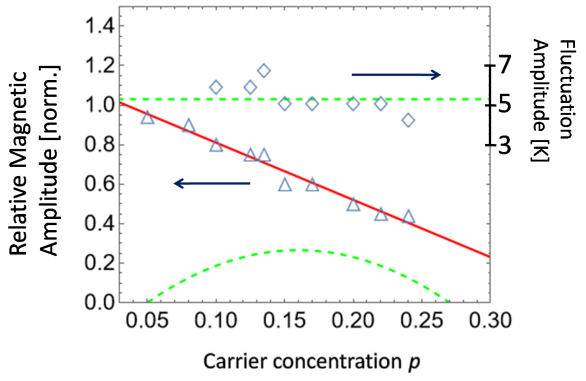

FIG. 18. (Color online) Relative magnetic amplitude $\frac{A_{mag}}{A_{mag}+A_{pair}}$ deduced from the fits of $\gamma(T)$ in $La_{2-x}Sr_xCuO_4$ and fluctuation temperature scale ΔT as a function of hole concentration p.

From the fits, we also find a novel linear dependence of the magnetic relative amplitude $A_{mag}/(A_{mag}+A_{pair})$ as a function of carrier concentration, which decreases from underdoped to overdoped sides of the phase diagram (see Fig. 18). However, the detailed shape of the entropy is still very sensitive to the parameters, in particular both the T_{max} and T^* values, which are much lower in the overdoped case, as shown in the phase diagram Fig. 14. This explains why the 'hump' in the background in $\gamma(T)$ is much closer to the critical temperature, and may be difficult to resolve without further analysis. These remarks help explain why the correct antinodal pseudogap is difficult to pinpoint in the specific heat, and indeed many other thermal/transport measurements, as compared to ARPES and tunneling. We thus give a clear response to the objections of Tallon et al. [25] who argue that, in the underdoped case, the entropy never recovers the normal state even at high temperature due to the pseudogap, contradicting the 'pairon' model.

The magnetic entropy of antiferromagnetic material has been given much attention [34, 39]. As discussed above, our results confirm that it changes significantly depending on the T_{max} value, which separates spin blocking to Curie-Weiss fluctuations. In the underdoped regime T_{max} is large (compared to T_c and T^*) and the effect of spin excitations on $\gamma(T)$ is such that it increases with temperature (strong AF correlations). At the opposite end of the dome, in the overdoped regime, T_{max} is much smaller and a Curie-Weiss law is responsible for the decrease of $\gamma(T)$ with temperature. These conclusions, independent of the pairon model, are in agreement with the overall background observed in $\gamma(T)$.

The case of YBCO

Our analysis for the two materials LSCO, single layer, and BSCCO, double layer, is consistent. The question now arises for the case of oxygen doped YBCO.

We then perform the same fitting procedure for oxygen doped YBCO, Fig. 19. As for LSCO, three temperature scales can be clearly distinguished above T_c: the pseudogap temperature T_Y^*, the magnetic temperature T_{max} and the fluctuation temperature T_{fluc}. Surprisingly, we find that the phase diagram, shown in Fig. 20, turns out to be different from the one obtained for LSCO. The two temperatures $T_Y^*(p)$ and $T_{max}(p)$, while remaining distinct, seem to converge towards the same point $p_c \approx 0.2$. and eventually vanish there.

The apparent pseudogap temperature deduced from the fits follows the line:

$$2.2\, k_B T_Y^*(p) \simeq 2.2\, k_B T^*(p) - A \times \left(\frac{p}{p_c}\right) \qquad (11)$$

where $A = 21.5$ is a constant, $p_c \simeq 0.2$ and $T^*(p)$ is the expected pseudogap temperature line (found for BSCCO). The results of the fits clearly show that YBCO

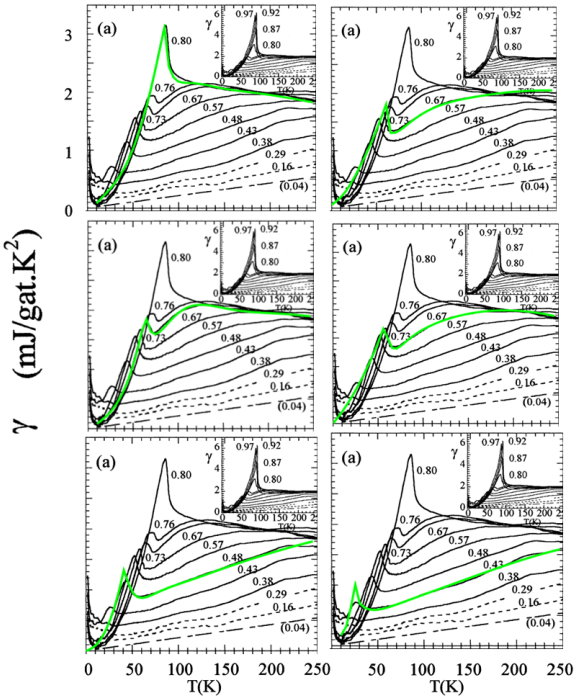

FIG. 19. (Color online) Experimental $\gamma(T)$ measured in $YBa_2Cu_3O_{7-\delta}$ (adapted from Ref. [15]) and corresponding fit calculated with the same phenomenological expression (green lines).

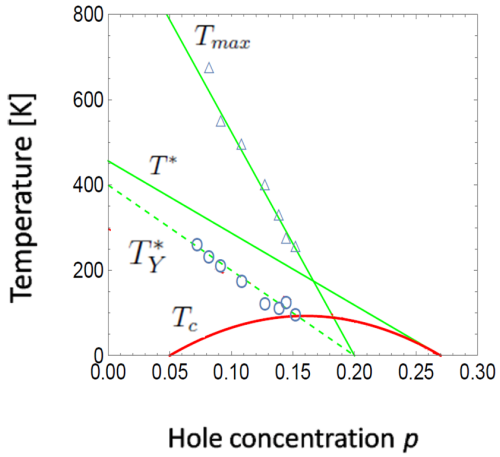

FIG. 20. (Color online) Phase diagram of $YBa_2Cu_3O_{7-\delta}$ deduced from the fits. Both lines $T_Y^*(p)$ and $T_{max}(p)$ seem to converge towards the critical value $p_c = 0.2$. Contrary to the two other materials, the $T_Y^*(p)$ line has a different behavior, as discussed in the text.

is different from the two other materials, although they mostly have the same relevant physical parameters. As is well known, YBCO is different in its structure (see [40] for a review); it is more isotropic than LSCO and BSCCO and has a combination of CuO planes and 1D chains [41]. In addition to the specific heat, both the magnetic susceptibility and resistivity show a different behavior, which remains controversial. The progressive filling of the oxygen chains parallel to the 2D CuO planes with oxygen doping may explain the unusual $T_Y^*(p)$ line. For example, this progressive filling could preferentially modify the Fermi-level gap along the nodal direction, hence leading to the modified law Eq.11. Further studies are necessary to resolve this apparent paradox.

Unconventional fluctuation regime

As noted previously, the specific heat appears to have a common signature of an unusually large exponential decay above the critical temperature. From the fits in LSCO and YBCO, we have extracted the characteristic temperature scale ΔT of the fluctuation regime above T_c. It is important to note that these fluctuations do not commence below T_c as in the model of Tallon et al.[42]. This effect is clearly illustrated in the present model in Figs. 8,9,10,11.

In view of the difference in T_c, it can be noted that $\Delta T \sim 5K$ for LSCO and twice that value for YBCO and BSCCO (see Fig. 18 for the case of LSCO). The scale of the fluctuation regime is therefore much larger than the BCS case (a few percent of T_c), see Fig. 2. Furthermore, ΔT hardly varies with doping and therefore $T_c + \Delta T$ follows the dome, as in Fig. 21. This finding is in qualitative agreement with the result of Tallon et al., although obtained with a different analysis [42].

Since the fluctuation regime is clearly unconventional, we suggest a novel mechanism. In the pairon model, the minimum hole density to have a condensate $p_{min} \simeq 0.05$, at the beginning of the T_c-dome, corresponds to one pairon every $\sim 6-7a_0$ where a_0 is the lattice constant. This is related in our model to the fundamental pairon-pairon interacting distance d_0, responsible for the condensation.

These considerations imply a new energy scale in the phase diagram:

$$2\delta_M \approx J_{eff} \times p_{min} \tag{12}$$

where J_{eff} is the effective antiferromagnetic exchange energy at $p = p_{min}$, Numerically, it gives the approximate value $2\delta_M \approx 3.8$ meV, clearly smaller than any previously mentioned energy scale.

On the other hand, as in the derivation of the entropy, it is necessary to have a minimum activation of a pairon from the condensate $\delta \sim 1-2$ meV due to the Bose-Einstein singularity in a 2D system [27]. A remarkable coincidence is that the mini-gap in the excitation spectrum is the same order of magnitude as the fluctuation energy δ_M described above. Hypothetically, these unconventional fluctuations are due to the activation of pairons in and out of the condensate across the mini-gap once the density has reached a critically small value. This is clearly in support of a new and important energy scale in cuprates, δ_M.

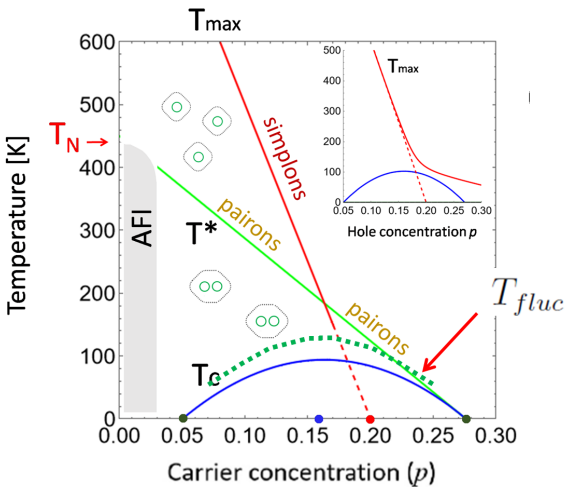

FIG. 21. (Color online) Generic phase diagram of $La_{2-x}Sr_xCuO_4$ and $Bi_2Sr_2CaCu_2O_{8+\delta}$ (the numerical values for T_c and T^* are the for $Bi_2Sr_2CaCu_2O_{8+\delta}$; the $T_{max}(p)$ line is for both materials). $T^*(p)$ is the characteristic temperature of magnetic correlations. Below T_{max}, 'simplons', one hole surrounded by 4 frozen spins are formed. Pairons form at the onset temperature T^*, the pseudogap temperature. They condensed below the critical temperature T_c. Above T_c, we indicate the unconventional fluctuation regime (as discussed in the text) on the scale ΔT, which follows the critical dome.

CONCLUSION

In this work, we revisit the specific heat of cuprates in the framework of the pairon model. In particular, we introduce a general expression for the temperature-dependent entropy. While no contradiction with the pairon model is found, our analysis strongly suggests that it is crucial to take into account the magnetic contribution.

The general shape of the cuprates entropy can be well described by the model. From precise fits for three different cuprates, LSCO, BSCCO and YBCO, we have deduced the three temperature scales are present above T_c in the phase diagram: the pseudogap temperature T^*, the magnetic temperature T_{max}, and the fluctuation temperature T_{fluct}. The resulting phase diagram is completely consistent with the one previously deduced from the magnetic susceptibility.

We show that a strong evolution of the entropy from the underdoped to the overdoped regime is mainly due to the contribution of the magnetic excitations and not to a T-independent gap in the electronic density of states. However, a temperature dependent pseudogap, consistent with a pairing gap, does exist throughout the phase diagram. Its temperature scale $T^*(p)$ for LSCO and BSCCO follows a linear behavior and vanishes and the end of the dome, in agreement with photoemission and tunneling spectroscopy. A different behavior is found for YBCO, where the apparent pseudogap temperature follows a steeper linear law and vanishes near $p_c \simeq 0.2$, similar to $T_{max}(p)$.

The fluctuation regime is found to be highly unconventional, the characteristic temperature scale of fluctuations being large and almost independent of carrier density. We relate this effect to the minimum doping value p_{min}, at the onset the T_c-dome. It is consistent with the mini-gap $\delta_M \sim 1-2meV$ in the pairon excitation energy spectrum that is required for the condensation mechanism. It is therefore a key energy scale of the problem.

ACKNOWLEDGEMENTS

The authors gratefully acknowledge discussions with Dr. Hiroshi Eisaki, Dr. Shigeyuki Ishida, Dr. Jeff Tallon, and Prof. Atsushi Fujimori.

[1] Hai-Hu Wen , Specific heat in superconductors, Chinese Phys. B **29** 017401 (2020).
[2] J. Bardeen, L. Cooper, J. Schrieffer, Theory of Superconductivity, Phys. Rev. **108** 1175 (1957).
[3] T. Klimczuk, M. Szlawska, D. Kaczorowski, J. R. O'Brien and D. J. Safarik, Superconductivity in the Einstein solid $VAl_{10.1}$, J. Phys.: Condens. Matter **24**, 365701 (2012).
[4] C. P. Moca and Boldizsár Jankó, Electronic specific heat in the pairing pseudogap regime, Phys. Rev. B **65**, 052503 (2002).
[5] Philippe Curty and Hans Beck, Thermodynamics and Phase Diagram of High Temperature Superconductors, Phys. Rev. Lett. **91**, 257002 (2003).
[6] A. J. H. Borne, J. P. Carbotte, and E. J. Nicol, Specific heat across the superconducting dome in the cuprates, Phys. Rev. **B 82**, 094523 (2010).
[7] J. W. Loram, K. A. Mirza, J. R. Cooper, and W. Y. Liang, Electronic specific heat of $YBa_2Cu_3O_{6+x}$ from 1.8 to 300 K, Phys. Rev. Lett. **71**, 1740 (1993).
[8] J.W.Loram, K.A.Mirza, J.M.Wade, J.R.Cooper, W.Y.Liang, The electronic specific heat of cuprate superconductors, Physica C **235–240**, Pages 134 (1994).
[9] Toshiaki Matsuzaki, Naoki Momono, Migaku Oda and Masayuki Ido, Electronic Specific Heat of $La_{2-x}Sr_xCuO_4$: Pseudogap Formation and Reduction of the Superconducting Condensation Energy, Journal of the Physical Society of Japan, **73**, 2232 (2004).
[10] Hai-Hu Wen, Gang Mu, Huiqian Luo, Huan Yang, Lei Shan, Cong Ren, Peng Cheng, Jing Yan, and Lei Fang, Specific-Heat Measurement of a Residual Superconducting State in the Normal State of Underdoped $Bi_2Sr_{2-x}La_xCuO_{6+\delta}$ Cuprate Superconductors, Phys. Rev. Lett. **103**, 067002 (2009).
[11] S. E. Inderhees, M. B. Salamon, T. A. Friedmann, and D. M. Ginsberg, Measurement of the specific-heat anomaly at the superconducting transition of $YBa_2Cu_3O_{7-\delta}$ Phys. Rev. B **36**, 2401(R) (1987).
[12] Y. Noat, A. Mauger, M. Nohara, H. Eisaki, W. Sacks , How 'pairons' are revealed in the electronic specific heat of cuprates, Solid State Communications **323**, 114109 (2021).

[13] S. E. Inderhees, M. B. Salamon, Nigel Goldenfeld, J. P. Rice, B. G. Pazol, D. M. Ginsberg, J. Z. Liu, and G. W. Crabtree, Specific heat of single crystals of $YBa_2Cu_3O_{7-\delta}$: Fluctuation effects in a bulk superconductor Phys. Rev. Lett. **60**, 1178 (1988);

[14] J.W.Loram, K.A.Mirza, J.R.Cooper, J.L.Tallon, Specific heat evidence on the normal state pseudogap, Journal of Physics and Chemistry of Solids **59**, 2091(1998).

[15] J.W. Loram, J. Luo, J.R. Cooper, W.Y. Liang, J.L. Tallon, Evidence on the pseudogap and condensate from the electronic specific heat, Journal of Physics and Chemistry of Solids **62**, 59 (2001).

[16] Jeffery L. Tallon, James G. Storey, Thermodynamics of the pseudogap in cuprates, Front. Phys. 10:1030616 (2022).

[17] Ø. Fischer, M. Kugler, I. Maggio-Aprile, C. Berthod and C. Renner, Scanning tunneling spectroscopy of the cuprates, Rev. Mod. Phys. **79**, 353 (2007).

[18] Makoto Hashimoto, Inna M. Vishik, Rui-Hua He, Thomas P. Devereaux and Zhi-Xun Shen, Energy gaps in high-transition-temperature cuprate superconductors, Nature Physics **10**, 483 (2014).

[19] A. A. Kordyuk, Pseudogap from ARPES experiment:Three gaps in cuprates and topological superconductivity, Low Temp. Phys. **41**, 319 (2015).

[20] S. Hüfner, M. A. Hossain, A Damascelli, and G. A. Sawatzky,Two gaps make a high-temperature superconductor?, Rep. Prog. Phys., **71**, 062501 (2008).

[21] Y. Noat, A. Mauger, M. Nohara, H. Eisaki, W. Sacks, Cuprates phase diagram deduced from magnetic susceptibility: what is the 'true' pseudogap line?, Solid State Communications **348–349**, 114689 (2022).

[22] J. B. Torrance, A. Bezinge, A. I. Nazzal, T. C. Huang, S. S. P. Parkin, D. T. Keane, S. J. LaPlaca, P. M. Horn, and G. A. Held, Properties that change as superconductivity disappears at high-doping concentrations in $La_{2-x}Sr_xCuO_4$, Phys. Rev. B **40**, 8872 (1989).

[23] M.Oda, H.Matsuki, M.Ido, Common features of magnetic and superconducting properties in Y-doped $Bi_2(Sr,Ca)_3Cu_2O_8$ and Ba(Sr)-doped La_2CuO_4, Solid State Communications **74**, 1321 (1990).

[24] T. Nakano, M. Oda, C. Manabe, N. Momono, Y. Miura, and M. Ido, Magnetic properties and electronic conduction of superconducting $La_{2-x}Sr_xCuO_4$, Phys. Rev. B **49**, 16000 (1994).

[25] Jeffrey L. Tallon and James G. Storey, Thermodynamics and the pairon model for cuprates, Phys. Rev. B **107**, 054507 (2023).

[26] W. Sacks, A. Mauger and Y. Noat, Cooper pairs without glue in high-T_c superconductors: A universal phase diagram, Euro. Phys. Lett **119**, 17001 (2017).

[27] W. Sacks, A. Mauger, Y. Noat, Pair – pair interactions as a mechanism for high-T_c superconductivity, Superconduct. Sci. Technol., **28** 105014 (2015).

[28] Yves Noat, Alain Mauger, William Sacks. Superconductivity in cuprates governed by topological constraints. Physics Letters A **444**, 128227 (2022).

[29] Yves Noat Alain Mauger, William Sacks, Statistics of the cuprate pairon states on a square lattice, Modelling Simul. Mater. Sci. Eng. **31**, 075010 (2023).

[30] William Sacks, Alain Mauger, and Yves Noat, Unconventional temperature dependence of the cuprate excitation spectrum, Eur. Phys. J. B **89**, 183 (2016).

[31] William Sacks, A. Mauger and Y. Noat, Origin of the Fermi arcs in cuprates: a dual role of quasiparticle and pair excitations, Journal of Physics: Condensed Matter, **30**, 475703 (2018).

[32] Yves Noat, Alain Mauger and William Sacks, Single origin of the nodal and antinodal gaps in cuprates, Euro. Phys. Lett **126**, 67001 (2019).

[33] Vitaly V. Kocharovsky, Vladimir V. Kocharovsky, Martin Holthaus, C.H. Raymond Ooi, Anatoly Svidzinsky, Wolfgang Ketterle, Marlan O. Scully, Fluctuations in Ideal and Interacting Bose-Einstein Condensates: From the Laser Phase Transition Analogy to Squeezed States and Bogoliubov Quasiparticles, Advances In Atomic, Molecular, and Optical Physics **53**, 291-411 (2006).

[34] M. E. Lines, The quadratic-layer antiferromagnet, J. Phys. Chem. Solids . **31**, 101 (1970).

[35] C. Girod, D. LeBoeuf, A. Demuer, G. Seyfarth, S. Imajo, K. Kindo, Y. Kohama, M. Lizaire, A. Legros, A. Gourgout, H. Takagi, T. Kurosawa, M. Oda, N. Momono, J. Chang, S. Ono, G.-q. Zheng, C. Marcenat, L. Taillefer, and T. Klein, Normal state specific heat in the cuprate superconductors $La_{2-x}Sr_xCuO_4$ and $Bi_{2+y}Sr_{2-x-y}La_xCuO_{6+\delta}$ near the critical point of the pseudogap phase, Phys. Rev. B **103**, 214506 (2021), and Michon, B., Girod, C., Badoux, S. et al., Thermodynamic signatures of quantum criticality in cuprate superconductors, Nature **567**, 218 (2019).

[36] S.H.Naqib, J.R.Cooper, Effect of the pseudogap on the uniform magnetic susceptibility of $Y_{1?x}Ca_xBa_2Cu_3O_{7?\delta}$, Physica C: Superconductivity **460–462**, 750-752 (2007).

[37] S H Naqib and R S Islam, Extraction of the pseudogap energy scale from the static magnetic susceptibility of single and double CuO_2 plane high-T_c cuprates,Supercond. Sci. Technol. **21**, 105017 (2008).

[38] R.S. Islam, M.M. Hasan, S.H. Naqib, Nature of the Pseudogap in High-T c Cuprates: Analysis of the Bulk Magnetic Susceptibility of La_{2-x} $Sr_xCu_{1-y}Zn_yO_4$, J. Supercond. Nov. Magn. **23**, 1569 (2010).

[39] L.J. de Jongh and A. R. Miedema, Experiments on simple magnetic model systems, Adv. Phys. **23**, 1 (1974).

[40] Roland Hott, Reinhold Kleiner, Thomas Wolf and Gertrud Zwicknag, Superconducting Materials – A Topical Overview, in Frontiers in Superconducting Materials, Ed. Anant V. Narlikar, Springer Verlag, Berlin, pp 1-69 (2004).

[41] M. A. Beno, L. Soderholm, D. W. Capone, D. G. Hinks, J. D. Jorgensen, J. D. Grace; Ivan K. Schuller, C. U. Segre; K. Zhang, Structure of the single phase high temperature superconductor $YBa_2Cu_3O_{7-\delta}$, Appl. Phys. Lett. **51**, 57 (1987).

[42] J. L. Tallon, J. G. Storey, and J. W. Loram, Fluctuations and critical temperature reduction in cuprate superconductors, Phys. Rev. B **83**, 092502 (2011).